



Pretreatment optimization of membrane-concentrated leachate through enhanced coagulation

Xu Ren^{a,*}, Hongbin Wang^a, Kai Song^{b,*}, Li Zeng^a, Jie Liu^a, Yangming Ou^a

^aSchool of Architecture and Civil Engineering, Chengdu University, No. 2025, Chengluo Road, Chengdu 610106, Sichuan, China, emails: renxu@cdu.edu.cn (X. Ren), wanghongbin@cdu.edu.cn (H. Wang), zengli512@126.com (L. Zeng), ouyangming@cdu.edu.cn (Y. Ou)

^bFaculty of Geosciences and Environmental Engineering, Southwest Jiaotong University, No. 111, North Section 1, 2nd Ring Road, Chengdu 610031, China, email: songkailw@163.com

Received 28 December 2020; Accepted 1 May 2021

ABSTRACT

Proper disposal of membrane-concentrated leachate (MCL) is problematic for municipal solid waste incineration (MSWI) plants. Many MSWI plants treat concentrated leachate using multistage processes, among which a pretreatment before advanced oxidation process (AOP) is the most common practice. In this study, four commonly used coagulants were applied to conduct enhanced coagulation pretreatment on a two-stage tight material MCL, which is collected from MSWI plants. Conditions of enhanced coagulation, including coagulant and its dosage (PSAF, 5 g L⁻¹), coagulant aid dosage (PAM, 80 mg L⁻¹), and initial pH (7), were determined through a single factor experiment. After pretreatment, the removal efficiency toward chemical oxygen demand (COD), UV absorption at 254 nm, total nitrogen, color, and turbidity were 80.6%, 89.0%, 97.8%, 17.0%, and 84.8%, respectively. Moreover, dissolved organic matter (DOM) characteristics before and after pretreatment were investigated via spectrum analyses in detail. UV-visible light and three-dimensional fluorescence analysis showed that the MCL was laden with refractory organic matter; concentration of DOM, especially that of humic-like acid, were deeply decreased after pretreatment. While flow field-flow fractionation measurements illustrated DOM molecular weight was just slightly reduced by the enhanced coagulation, and it was challenging for the enhanced coagulation to change the DOM molecular weight distribution. Finally, the results of gas chromatography-mass spectrometry analysis were illustrated that the main types of volatile organic compounds (VOCs) in MCL were chain organic compounds and some aromatic compounds with relatively low molecular weight, and they were easily removed or decomposed through enhanced coagulation. This study provides a theoretical basis for the enhanced coagulation for pretreatment of MCL.

Keywords: Municipal solid waste incineration; Membrane-concentrated leachate; Enhanced coagulation; Optimization; DOM characteristics

1. Introduction

Due to the Chinese Government's encouragement, ≈46% of municipal solid waste (MSW) treatment has been by incineration (China Statistical Yearbook [1]). As a result, the municipal solid waste incineration (MSWI) capacity in China has increased by 4.12 times in the past

decade. Usually, large leachate quantities are generated in MSWI plants due to MSW's high moisture content, often treated by combining biochemical and membrane systems [2]. About 15%–30% of the leachate is converted to membrane-concentrated [3,4] which is a real headache issue of municipal MSWI plants because it contains various and extremely high concentrations of pollutants (especially

* Corresponding authors.

organics) [3]. As a solution, many MSWI plants recirculate membrane-concentrated leachates (MCL) into a leachate treatment system, which is relatively easy to operate [5]. However, a resulting problem whereby scales block the membrane, leading to leachate breakdown occurs. Therefore, recirculation was gradually phased out, and most plants prefer to decompose the MCL by incineration. Yet, spraying aggravates the corrosion of the incineration and flue gas purification systems. Moreover, because some plants cannot contain the spraying volume, the excess concentrated leachate in the MSWI plants has to be transferred to other wastewater treatment plants with some economic and environmental risks. Therefore, effective treatment of MCL is crucial to achieving zero-release of pollution in MSWI plants.

So far, no single treatment has shown a benign process for MCL control. However, including a pretreatment step before the main treatment process [6] (e.g., advanced oxidation process (AOP) [7,8]) has proven efficient. In this case, coagulation is the most commonly used pretreatment due to its numerous merits [9,10], such as relatively high efficiency [11], low-cost, and easy operation [10,12]. In recent years, enhanced coagulation has been popularly applied as the pretreatment of leachate [13–15]. An improved removal efficiency over the traditional coagulation process was reported [16–18].

In our previous study, we found that polymeric aluminum (PAC), aluminum sulfate ($Al_2(SO_4)_3$), polyaluminum ferric chloride (PAFC), and polyferrosilicate aluminum (PSAF) evinced enhanced performance against organic-laden wastewaters. Further, this current study optimized the enhanced coagulation process of organics by varying some parameters (such as the coagulant and its dosage, coagulant dosage, and initial pH) in a two-stage tight material (TSTM) MCL from an MSWI plant. Thence, suitable water quality for further treatment could be obtained. Concurrently, the dissolved

organic matter (DOM) in the MCL before and after enhanced coagulation were characterized via spectral analyses.

2. Materials and methods

2.1. Samples

The pristine MCL was collected from the leachate treatment system of the MSWI plant in the northeast of the Chengdu basin. Therein, nanofiltration membrane (NF), reverse osmosis (RO) membrane, and TSTM membrane system are used together in the advanced treatment unit. The TSTM membrane system can reduce the nanofiltration MCL volume by isolating the DOM (especially refractory organics), thereby concentrating the pollutants (Fig. 1). The characteristics of raw samples are provided in Table 1.

2.2. Reagents

The four coagulants: PAC (purity $\geq 30\%$), $Al_2(SO_4)_3$ (analytical purity), PAFC (purity $\geq 35\%$), and PSAF (purity $\geq 27\%$), whose performance was studied, were purchased from Teng-Long Waste Water Treatment Materials Co., Ltd., (Gongyi City, Henan Province of China). Cationic polyacrylamide (PAM, ion exponent = 35%–55%), purchased from Ke-Long Chemical Factory in Chengdu City of China was chosen as the coagulant aid. Ultrapure water, with a resistance of $18.25\text{ M}\Omega\text{ cm}^{-1}$, was used for all the analyses.

2.3. Experimentation

After adjusting the initial pH, certain doses of the coagulants and coagulant aid were added to the pristine MCL under stirring. The optimal condition was determined by a single factor experiment. Chemical oxygen demand (COD), UV absorption at 254 nm (UV_{254}), solution conductivity

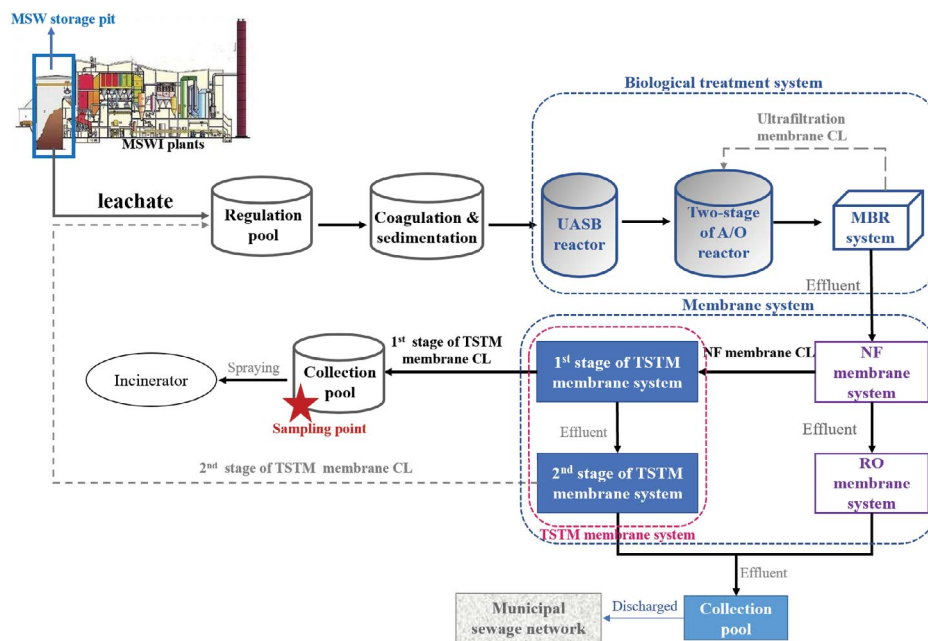


Fig. 1. Leachate treatment process and the sampling point.

Table 1
Characteristics of TSTM membrane-concentrated leachate before and after enhanced coagulation

Item	COD (mg L ⁻¹)	UV ₂₅₄ (AU cm ⁻¹)	NH ₃ -N (mg L ⁻¹)	TN (mg L ⁻¹)	CN (PCU)	TUB (NTU)	SC (mS cm ⁻¹)	pH
Pristine MCL	9,500	118	428	1,550	25,500	191	39.9	7.47
Pretreated MCL	1,840	13.0	636	1,290	550	29.2	47.7	4.62
*Re (%)	80.6	89.0	-48.5	17.0	97.8	84.8	-19.6	38.2

*Re = percentage reduction in each indicator values compared to pristine MCL.

(SC), and color number (CN) were used to characterize the organics in the sample. Thus, the removal efficiencies of the systems were determined. Meanwhile, the removal of ammonia nitrogen (NH₃-N), total nitrogen (TN), turbidity (TUB), and sludge volume reduction were also evaluated to determine the optimal conditions of the coagulation.

2.4. Analysis methods

The COD, NH₃-N, TN, and TUB were determined using standard methods (APHA [19]). A pH meter (PHS-3C, Lei-ci, Shanghai, China) monitored the pH. At the same time, CN and SC were assessed with a colorimeter (SD9011, Xin-Rui, Shanghai, China) and conductivity meter (Hi8731n, HANNA Instruments Srl, Italy), respectively. Further analyses included DOM characterization (before and after enhanced coagulation) using four spectral analyses: ultraviolet-visible (UV-vis) light absorption spectrum, three-dimension excitation-emission matrix (3D-EEM), fluorescence spectrum and field-flow fractionation (FIFFF), and gas chromatography-mass spectrometry (GC-MS). Detailed analytical procedures were provided in our previous studies [4,5].

3. Results and discussions

3.1. Optimization of coagulants

3.1.1. Polymeric aluminum

First, we carried out a preliminary experiment to establish the relatively efficient dosage range of the coagulant. Then, various dosages of each coagulant and 5 mg of coagulant aid (PAM) were added to 100 mL of the pristine MCL in turn. After the coagulation, the extent of pollutant removal was calculated to determine the optimal coagulant and dosage.

Fig. 2a shows that the removal of COD, UV₂₅₄ and CN increased with PAC dosage. The PAC dosage of 30 g L⁻¹ achieved the optimal removal efficiency for COD (72.0%), UV₂₅₄ (84.6%), and CN (89.4%). A remarkable finding (Fig. 2) was that all the coagulants exhibited abysmal removal efficiency toward NH₃-N, even increasing the NH₃-N concentration in pretreated samples. According to the theory of a double electrical layer of colloidal particles, with aluminum/iron salt coagulants, the colloids showed a strong attraction for negatively charged contaminants, while the NH₃-N likely originated from NH₄⁺ under acidic conditions. Hence, coagulation was ineffective for its removal. Besides, three coagulants were

of industrial-grade purity, their levels of impurities may induce an increase in NH₃-N concentration.

3.1.2. Aluminum sulfate

Fig. 2b shows that by increasing Al₂(SO₄)₃ dosage, the removal of COD, UV₂₅₄ and CN decreased mildly. Al(OH)₃ formed in the solutions after adding Al₂(SO₄)₃ polymerizing to Al_n(OH)_{3n} colloids, which readily combine with negatively charged pollutants. However, excessive coagulant dosage changed the surface charge of the colloids, preventing Al_n(OH)_{3n} colloid formation, thereby decreasing the pollutants removal. With 5 g L⁻¹ coagulant dosage, the removal of COD, UV₂₅₄ and CN reached 47.9%, 64.3%, and 83.14%, respectively. However, when upped to 30 g L⁻¹, they lowered to 41.2%, 53.9%, and 77.7%, respectively. Compared with the other coagulants, the Al₂(SO₄)₃ removal efficiency was inferior. Therefore, Al₂(SO₄)₃ was not the preferred coagulant for treating MCL.

3.1.3. Polyaluminum ferric chloride

Compared with PAC and Al₂(SO₄)₃, PAFC exhibited superior removal efficiency toward COD, UV₂₅₄ and CN (Fig. 2c). Besides, the flocs generated by PAFC coagulation were larger, making their removal faster and cleaner. The removal of COD, UV₂₅₄, CN, and TUB increased with ≤25 g L⁻¹ PAFC dosage, at which the respective optimal removal efficiencies of 66.9%, 81.2%, 95.0%, and 67.3% were achieved. However, at 25 g L⁻¹ dosage, the removal efficiency declined. NH₃-N concentration increased due to system pH decreased after coagulation. Additionally, positively charged colloids could not adsorb NH₄⁺ effectively. Moreover, impurities contained in the industrial-grade coagulants could have contributed to the elevated NH₃-N levels. Overall, 25 g L⁻¹ was the most effective PAFC dosage, at which the sludge volume was 55 mL.

3.1.4. Polyferrosilicate aluminum

Relatively large floc particles were formed after adding PSAF to pristine MCL samples. The flocs sink and settle rapidly, and the sludge volume increased with PASF dosage. Overall, PASF showed the best removal efficiency toward COD, UV₂₅₄ and CN (Fig. 2d). The removal of TUB and CN was optimized at 50 g L⁻¹ PSFAF dosage. The performance depreciated slightly when the dosage was increased, owing to the PASF and PAM dosage mismatch. However, amongst the coagulants, PASF exhibited the worst removal efficiency

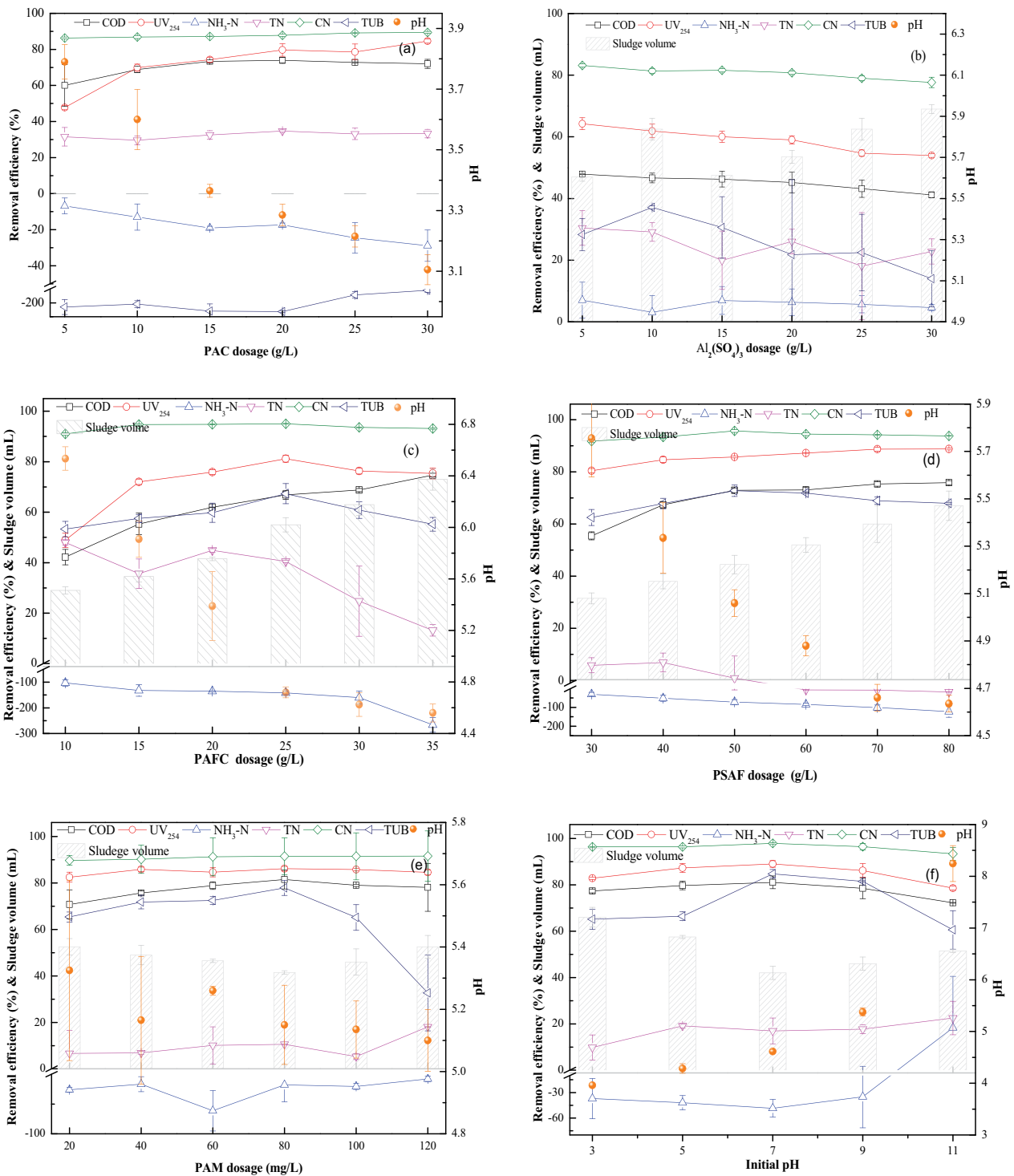


Fig. 2. Effects of coagulant and coagulant aid dosages: (a) PAC, (b) $Al_2(SO_4)_3$, (c) PAFC; (d) PSAF, and (e) PAM on the membrane-concentrated leachate removal and sludge volume reduction, (f) the effect of initial pH on pollutants' removal.

for TN, likely due to the dissolution of nitrogenous impurities in the sample. PASF was more effective at the optimal dosage than PAFC in removing organics, producing less sludge and larger-sized flocs. Therefore, 50 g L⁻¹ optimal dosage achieved 73.1%, 87.2%, and 94.5% removal of COD, UV₂₅₄ and CN, respectively.

The removal mechanisms of the pollutants are as follows: Aluminum salts (Al(III), from PSAF) hydrolyzed to form mononuclear complexes (such as $Al(OH)^{2+}$, $Al(OH)_2^+$, AlO_2^-). Subsequently, reactions occurred between these mononuclear complexes to form polynuclear complexes, $Al_n(OH)_m^{(3n-m)+}$ ($n > 1, m \leq 3n$) [20,21]:

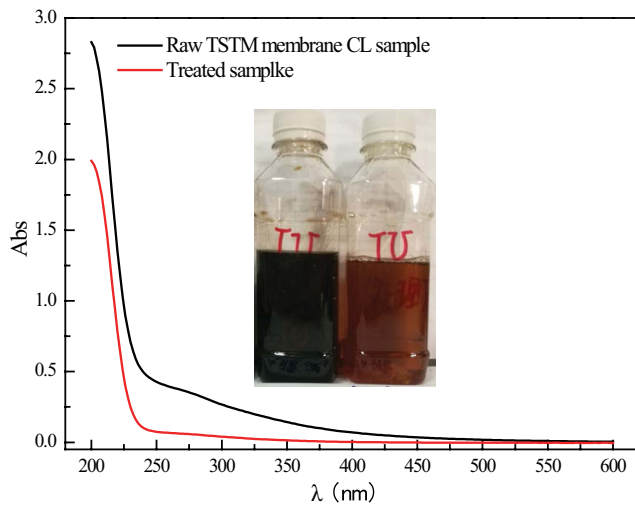
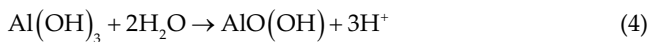
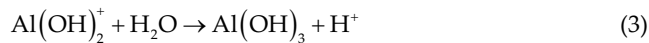
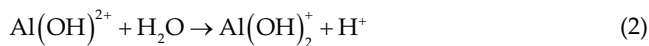
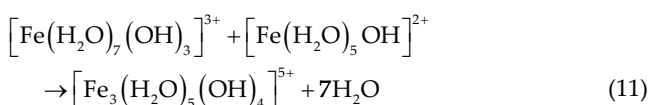
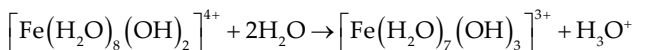
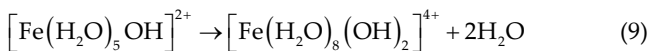
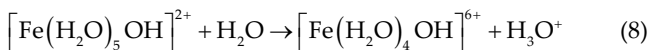
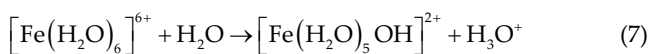
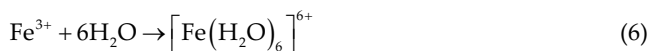


Fig. 3. UV-vis spectra of the test samples before and after enhanced coagulation.



Meanwhile, ferric salts (Fe(III), from PSAF) can also react in solutions as follows [22,23]:



The positive charge of these complexes enables prompt reaction with negatively charged contaminants. Generally,

contaminants can be removed through double-layer compression, adsorption electric neutralization, bridging between particles, precipitate particle entrapment, absorption, and sweep coagulation [24].

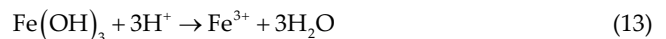
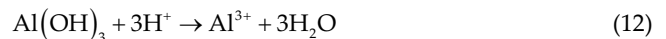
3.2. Dosage of coagulant aid

The pollutant removal or floc size can be improved by adding coagulant aids. One of such is PAM, with a high molecular weight. It promotes adsorption and bridging during coagulation [3]. With PAM dosages (20–120 mg L⁻¹), 5 g L⁻¹ of PSAF, and unaltered pH, PAM showed no significant effect on removing COD, UV₂₅₄ and CN. However, it improved on the supernatant TUB and sludge volume (Fig. 2e). Both properties decreased with the increase in PAM dosage of 80 mg L⁻¹, after which they started to increase due to a mismatch in dosage ratio between PSAF and PAM. Thus, 5 g L⁻¹ and 80 mg L⁻¹ were the respective optimum PSAF and PAM dosages, that is, the optimal dose-ratio of PSAF and PAM ($D_{\text{PSAF}}:D_{\text{PAM}}$) was 625:1. Here, the removal efficiencies for COD, UV₂₅₄, CN, and TUB were 81.52%, 86.14%, 91.47%, and 77.88%, respectively, while the sludge volume reduction was 41.5 mL.

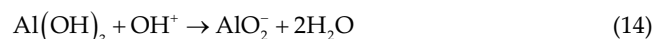
3.3. Effect of initial pH

We further investigated the influence of pH on the coagulation of MCL (with 5 g L⁻¹ of PSAF and 80 mg L⁻¹) of PAM in the pH range of 3–11. As depicted in Fig. 2f, the pollutants removal, especially the organics, were relatively low under extreme pHs, that is, at pH = 3 or 11. We ascribe such occurrence to the difficulty of coagulant to aggregate into large flocs under strongly acidic or alkaline conditions [Eqs. (12)–(14)]. For instance, the majority of Al species from PSAF would exist as Al³⁺ in strong acid conditions, with no removal abilities toward pollutants. During the experiment, numerous tiny particles were observed at the initial pHs 3 and 11. This is due to the flocs may disintegrate when the pH value is too high or low. Moreover, these specs could not settle easily, thereby increasing the TUB of the supernatant. At an initial pH of 7, COD, UV₂₅₄, CN, and TUB evinced the highest removal efficiencies of 81.1%, 89.0%, 97.8%, and 84.8%, respectively. Meanwhile, the pH, the average sludge volume was the least (i.e., 42 mL).

Strong acidic conditions:



Strong alkaline conditions:



In general, PSAF was the optimal coagulant for MCL, while the optimal conditions included adjusting pH to 7. After that, PSAF and PAM ($D_{\text{PSAF}}:D_{\text{PAM}} = 625:1$) were added with rapid stirring (300 rpm) for 60 s before lowering the speed to 60 rpm for 30 min. Finally, the mixture is left standing for 30 min before separating the supernatant by filtering.

3.4. Characteristics of DOM

3.4.1. UV-vis light absorption spectrum analysis

DOM, as a heterogeneous mixture [25], is the primary source of COD in MCL. Due to membrane interception, it contains many macromolecular organics with complex structures. Chen et al. [26,27] proved that MCL contains several refractory DOM types, with a high proportion of heteroatomic DOM that hinders biodegradation of MCL.

Many conjugated structures in refractory DOM [28], such as the aromatic nucleus, ethylene linkage, carboxyl, etc., have strong absorption at 200–380 nm [29]. These conjugated structure contains several chromophores (e.g., C=C and C=C and benzene ring) and auxochroic groups (e.g., -X and -OR). As shown in Fig. 3, the samples before and after treatment showed strong absorptions in the UV region. However, the pretreated sample's spectra evinced a blue shift, and the absorbance reduced significantly in the UV region. These observations show that enhanced coagulation can remove some chromophores and auxochroic groups.

Usually, absorbance or absorbance ratio at specific wavelengths are used to illustrate the characteristics of specific DOMs. For instance, absorptions at 254 nm (E_{254}) and 280 nm (E_{280}) are characteristic of refractory DOMs, such as aromatic organics. The E_{250}/E_{365} ratio is related to the DOM molecular weight; the smaller the value, the larger the molecular weight of DOM. Moreover, E_{300}/E_{400} is inversely proportional to molecular weight, humus degree, and aromaticity of DOM. As illustrated in Table 2, E_{254} and E_{280} decreased after the enhanced coagulation, showing the reduction of refractory DOM in the sample. Similarly, an increase in E_{250}/E_{365} and E_{300}/E_{400} indicates a lower average molecular weight of DOM. In summary, the enhanced coagulation can remove some refractory DOM in the pristine MCL. It may also break the unsaturated bonds of the DOM, thereby reducing the average molecular weight of the DOM in the sample.

3.4.2. 3D-EEM fluorescence spectrum analysis

3D-EEM fluorescence spectrum is widely used to identify fluorescent DOM [30], such as humic-like, tyrosine-like,

Table 2

UV-vis analysis results of the test samples before and after enhanced coagulation

Sample	E_{254}	E_{280}	E_{250}/E_{365}	E_{300}/E_{400}
Pristine MCL	0.412	0.338	3.76	3.838
Pretreated MCL	0.071	0.555	7.96	30.3

tryptophan-like, or phenol-like organic compounds. Moreover, the analysis correlates the position, shift, and intensity of fluorescence peaks to DOM structural information and concentration [31,32]. According to Chen et al. [25], 3D-EEM fluorescence spectrum can be divided into five regions for DOM characterization: region I ($E_x < 250$ nm, $E_m < 330$ nm) and region II ($E_x < 250$ nm, 330 nm $< E_m < 380$ nm), both related to the simple aromatic protein; region III ($E_x < 250$ nm, $E_m > 380$ nm) represents fulvic-like acid; region IV ($E_x > 250$ nm, $E_m > 380$ nm) indicates the fluorescence spectrum of humic-like acid; region V (250 nm $< E_x < 280$ nm, $E_m < 380$ nm) represents the by-products of microbial metabolic.

Fig. 4 shows the 3D-EEM fluorescence spectrum of the samples before and after enhanced coagulation. In Fig. 4a, we observed two peaks (peak 1 (E_x/E_m , 250/460 nm) in region III and peak 2 (E_x/E_m , 240/480 nm) in region IV), related to the fulvic-like acid and humic-like acid, respectively. After the enhanced coagulation, the spectra exhibited a blue shift, and all the intensities of the various regions decreased significantly, indicating that the DOM composition had changed. However, two relative strong peaks identified in regions II and III, that is, peak 1 (E_x/E_m , 240/480 nm) and peak 2 (E_x/E_m , 230/360 nm), were ascribed to fulvic-like and simple aromatic protein in treated sample (Fig. 4b). Furthermore, the signal intensity weakened in region IV, indicating that the humic-like acid concentration decreased significantly after the enhanced coagulation.

3.4.3. DOM molecular weight analysis

The FIFFF results of the continuous distribution of DOM molecular weight are depicted in Fig. 5. In a sequence, the

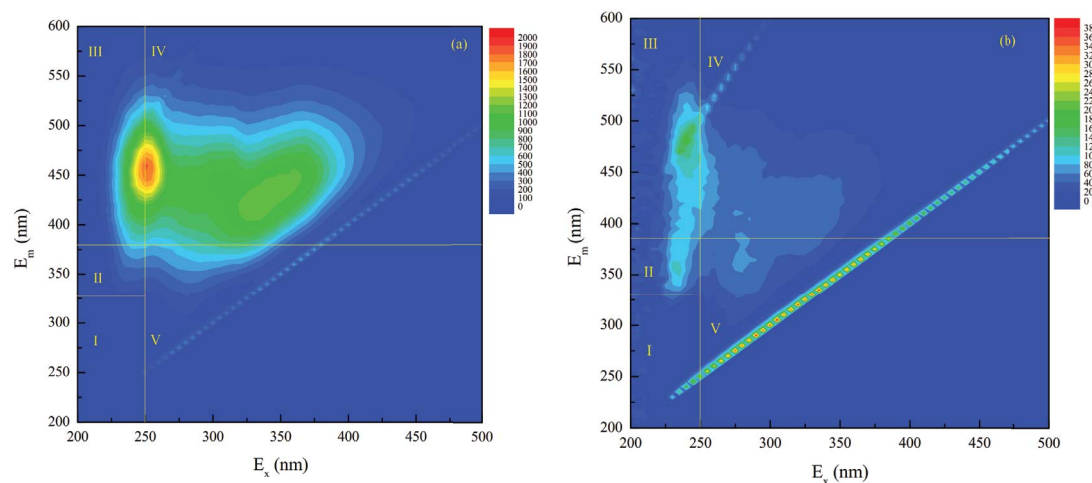


Fig. 4. 3D-EEM spectra of the (a) pristine MCL and (b) pretreated MCL.

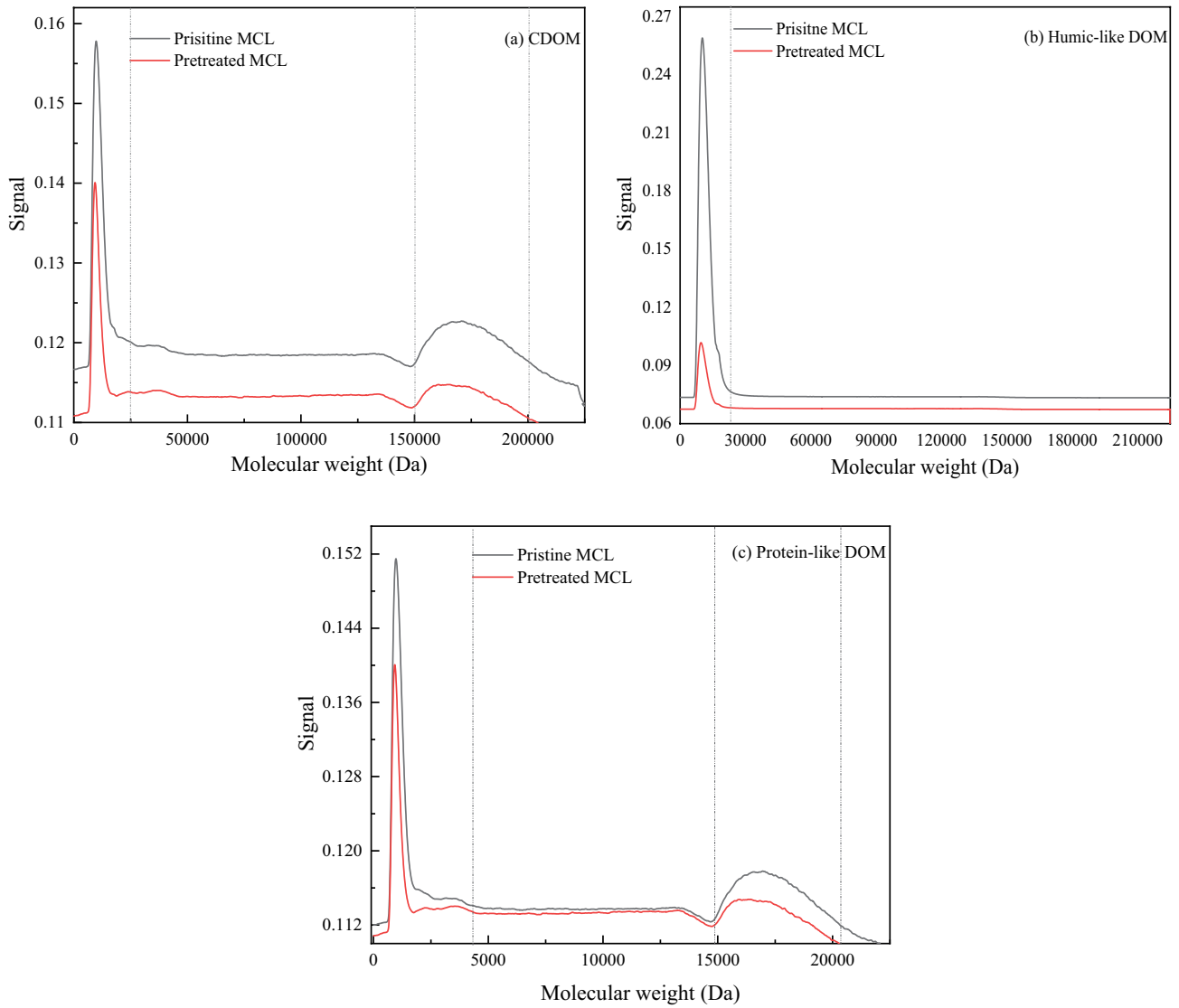


Fig. 5. FIFFF results of pristine MCL and pretreated MCL.

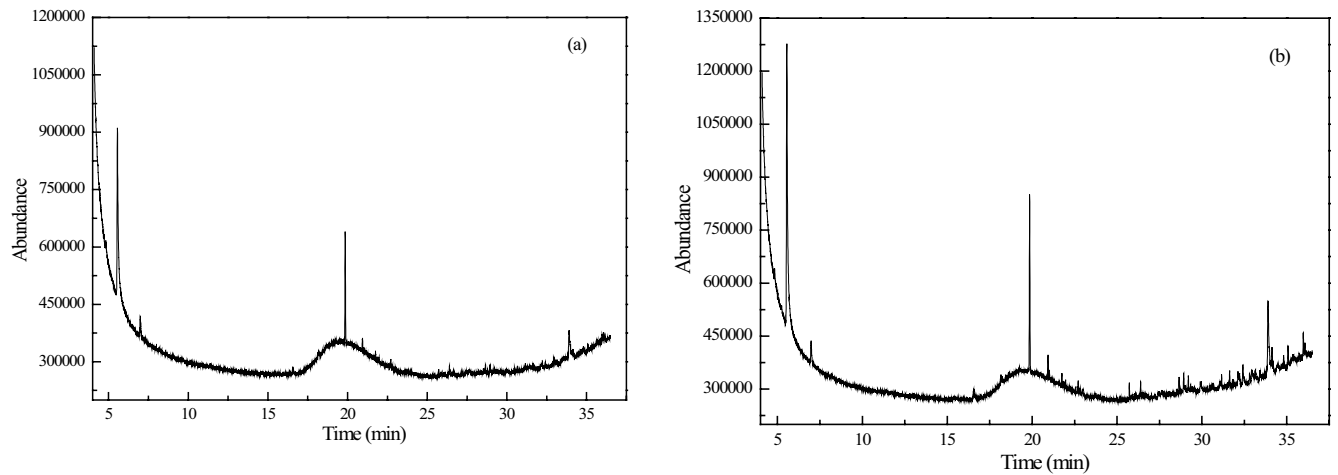


Fig. 6. Results of GC-MS analysis: (a) pristine MCL, (b) MCL pretreated.

samples passed through three detectors [33]: UV light detector ($\lambda = 254 \text{ nm}$), fluorescence detector I ($E_x/E_m = 350/450 \text{ nm}$), and fluorescence detector II ($E_x/E_m = 275/340 \text{ nm}$). According to Xu et al. [33], the spectra obtained from these detectors can, respectively, illustrate the molecular distribution of three DOM species: colored DOM (CDOM), humic-like DOM (HDOM), and protein-like DOM (PDOM). Here, although the spectra of CDOM, HDOM, and PDOM of the pristine MCL and pretreated MCL were similar, the signal intensities significantly decreased and the range of strong signal regions also narrowed slightly after pretreatment, illustrating that the concentration of three DOM species were decreased, while molecular weight was slightly reduced by the enhanced coagulation.

Regarding CODM, two distinct peaks were located at the molecular weight of 2,000–25,000 Da and 150,000–200,000 Da. The molecular weight of HDOM was mainly distributed in 7,500–22,500 Da, while those of PDOM were concentrated in two ranges: 500–4,000 Da and 15,000–20,000 Da. In terms of signal intensity, CDOM, HDOM, and PDOM with the respective molecular weight less than 25,000; 22,500; and 4,000 Da had higher concentrations than other weight ranges.

3.4.4. GC-MS analysis

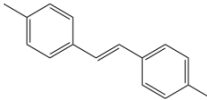
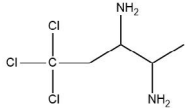
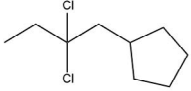
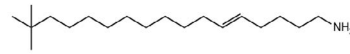
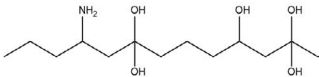
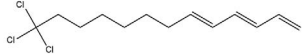
Refractory organics, including humic-like and fulvic-like substances, are the main types of organics in MCL [34]. Although the complexities of the structure of refractory organics in MCL have posed major challenges to accurately analyze the types of organics, several techniques can help us directly or indirectly speculate the possible

presence of organics in MCL. In this study, GC-MS analysis was applied to analyze the possible existence of volatile organic compounds (VOCs) in samples, so as to analyze the characteristics of organics before and after enhanced coagulation. It can be seen from Fig. 6 and Table 3, 21 and 6 types of organics were detected in pristine and pretreated MCL, respectively. Their molecular mass ranges from 200 to 400, which were much lower than humic-like and fulvic-like substances. The main types of VOCs were chain organic compounds and some aromatic compounds with relatively low molecular weight. Moreover, these organics with lower molecular weight and simple molecular structures might be easily removed or decomposed by enhanced coagulation, hence the organics types were decreased while some new organics types were detected in pretreated MCL.

4. Conclusions

The optimal conditions of the enhanced coagulation to treat TSTM MCL included pH adjustment of the leachate to 7. Also, PSAF and PAM are added ($D_{\text{PSAF}}:D_{\text{PAM}}$) in 625:1. After the enhanced coagulation, the system's optimal removal efficiency against COD, UV_{254} , CN, and TUB was 81.07%, 89.02%, 97.84%, and 84.75%, respectively. The organics removed through double-layer compression, adsorption electric neutralization, bridging between particles, particle entrapment via precipitation and absorption, and sweep coagulation. Generally, the concentrations of DOM, especially that of humic-like acid, decreased by the treatment. The organics with relatively low molecular mass and simple molecular structures were removed or decomposed through enhanced coagulation. However, it was challenging

Table 3
Possible organics in samples

Samples	Time	m/z	M_w	Molecular formula	Molecular structure
	5.553	207.0	208	$\text{C}_{16}\text{H}_{16}$	
	6.983	207.0	205.35	$\text{C}_5\text{H}_{11}\text{N}_2\text{Cl}_3$	
Pristine MCL	18.164	207.0	208.9	$\text{C}_{10}\text{H}_{18}\text{Cl}_2$	
	19.856	281.0	281	$\text{C}_{19}\text{H}_{39}\text{N}$	
	20.935	280.9	280	$\text{C}_{13}\text{H}_{30}\text{NO}_5$	
	21.757	281.1	281.35	$\text{C}_{13}\text{H}_{19}\text{Cl}_3$	

(Continued)

Table 3 Continued

Samples	Time	m/z	M_w	Molecular formula	Molecular structure
	25.728	207.0	206	$C_{15}H_{26}$	
	26.395	341.0	341	$C_{21}H_{41}O_3$	
	28.655	398.8	398	$C_{26}H_{54}O_2$	
	28.926	205.2	204	$C_{15}H_{24}$	
	29.202	169.1	170	$C_{12}H_{26}$	
	31.165	281.2	280.45	$C_{14}H_{29}O_3Cl$	
	31.636	281.0	280	$C_{19}H_{39}O$	
	32.125	280.0	280	$C_{18}H_{32}O_2$	
	32.413	355	354	$C_{19}H_{34}N_2O_4$	
	32.942	281.0	280	$C_{20}H_{40}$	
	33.897	305.2	304	$C_{18}H_{24}O_4$	
	34.132	281.1	280	$C_{20}H_{40}$	
	35.074	340.9	340	$C_{20}H_{42}O$	
	35.971	355.1	354	$C_{24}H_{50}O$	
	35.074	356.9	356	$C_{23}H_{48}O_2$	
	5.522	207.1	206	$C_{13}H_{18}O_2$	
	6.952	206.9	205.9	$C_9H_{13}NCl_2$	
Pretreated MCL	19.847	281.0	280	$C_{19}H_{38}N$	
	23.156	207.1	206	$C_{10}H_{22}O_4$	
	33.901	355.0	354	$C_{17}H_{26}O_6N_2$	
	36.069	355	355	$C_{26}H_{43}$	

for the enhanced coagulation to change the DOM molecular weight distribution, the next research should focus on promoting the decomposition of the macromolecular organics.

Acknowledgments

This study was supported by the Science and Technology Department of Sichuan province of China (Fund No. 2021YFS0290).

References

- [1] National Bureau of Statistics, Chinese Statistical Yearbook, 2019.
- [2] W.M. Chen, Y.F. Luo, G. Ran, Q.B. Li, An investigation of refractory organics in membrane bioreactor effluent following the treatment of landfill leachate by the O_3/H_2O_2 and MW/PS processes, *Waste Manage.*, 97 (2019) 1–9.
- [3] Y.Y. Long, J. Xu, D.S. Shen, Y. Du, H.J. Feng, Effective removal of contaminants in landfill leachate membrane concentrates by coagulation, *Chemosphere*, 167 (2017) 512–519.
- [4] X. Ren, X.M. Xu, Y. Xiao, W.M. Chen, K. Song, Effective removal by coagulation of contaminants in concentrated leachate from municipal solid waste incineration power plants, *Sci. Total Environ.*, 685 (2019) 392–400.
- [5] X. Ren, K. Song, Y. Xiao, S.Y. Zong, D. Liu, Effective treatment of spacer tube reverse osmosis membrane concentrated leachate from an incineration power plant using coagulation coupled with electrochemical treatment processes, *Chemosphere*, 244 (2020) 1–11, doi: 10.1016/j.chemosphere.2019.125479.
- [6] M. Moradi, F. Ghanbari, Application of response surface method for coagulation process in leachate treatment as pretreatment for Fenton process: biodegradability improvement, *J. Water Process Eng.*, 4 (2014) 67–73.
- [7] H.D. Qin, H.L. Chen, Pretreatment of concentrated leachate by the combination of coagulation and catalytic ozonation with Ce/AC catalyst, *Water Sci. Technol.*, 73 (2016) 511–519.
- [8] A.R. Ishak, F.S. Hamid, S. Mohamad, K.S. Tay, Stabilized landfill leachate treatment by coagulation-flocculation coupled with UV-based sulfate radical oxidation process, *Waste Manage.*, 76 (2018) 575–581.
- [9] E. Maranon, L. Castrillon, Y.F. Nava, A.F. Mendez, A.F. Sanchez, Coagulation-flocculation as a pretreatment process at a landfill leachate nitrification-denitrification plant, *J. Hazard. Mater.*, 156 (2008) 538–544.
- [10] D. Weblar, C.F. Mahler, M. Dezotti, Leachate treatment by combined processes: coagulation/flocculation, air stripping, ozonation and activated sludge, *Eng. Sanit. Ambiental*, 23 (2018) 901–911.
- [11] K. Luo, Y. Pang, X. Li, F. Chen, X. Liao, M. Lei, Y. Song, Landfill leachate treatment by coagulation/flocculation combined with microelectrolysis-Fenton processes, *Environ. Technol.*, 40 (2019) 1862–1870.
- [12] F. Ghanbari, J. Wu, M. Khatebasreh, D. Ding, K.Y.A. Lin, Efficient treatment for landfill leachate through sequential electrocoagulation, electrooxidation and PMS/UV/CuFe₂O₄ process, *Sep. Sci. Technol.*, 242 (2020) 3–8, doi: 10.1016/j.seppur.2020.116828.
- [13] M. Assou, L.E. Fels, A.E. Asli, H. Fakidi, S. Souabi, M. Hafidi, Landfill leachate treatment by a coagulation-flocculation process: effect of the introduction order of the reagents, *Desal. Water Treat.*, 57 (2016) 21817–21826.
- [14] R.G.S.M. Alfaia, M.M.P. Nascimento, D.M. Bila, J.C. Campos, Coagulation/flocculation as a pretreatment of landfill leachate for minimizing fouling in membrane processes, *Desal. Water Treat.*, 159 (2019) 53–59.
- [15] B. Aftab, J. Cho, H.S. Shin, J. Hur, Using EEM-PARAFAC to probe NF membrane fouling potential of stabilized landfill leachate pretreated by various options, *Waste Manage.*, 102 (2020) 260–269.
- [16] J.Y. Guo, Pretreatment of landfill leachate by using the composite of poly ferric sulfate and bioflocculant MBFR10543, *Desal. Water Treat.*, 57 (2016) 19262–19272.
- [17] K. Djefal, S. Bouranene, P. Fievet, S. Deon, A. Gheid, Treatment of controlled discharge leachate by coagulation-flocculation: influence of operational conditions, *Sep. Sci. Technol.*, 56 (2019) 168–183.
- [18] S.Y. Cheng, P.-L. Show, J.C. Juan, J.-S. Chang, B.F. Lau, S.H. Lai, E. Poh, Ng, H.C. Yian, T.C. Ling, Landfill leachate wastewater treatment to facilitate resource recovery by a coagulation-flocculation process via hydrogen bond, *Chemosphere*, 262 (2021) 1–4, doi: 10.1016/j.chemosphere.2020.127829.
- [19] APHA, Standard Method for the Examination of Water and Waste Water, 21st ed., American Public Health Association, Washington DC, 2005.
- [20] A. Tatsi, A.I. Zouboulis, K.A. Matis, P. Samaras, Coagulation-flocculation pretreatment of sanitary landfill leachate, *Chemosphere*, 53 (2003) 737–744.
- [21] Z.N. Shu, Y.P. Lu, J. Huang, W.H. Zhang, Treatment of compost leachate by the combination of coagulation and membrane process, *Chin. J. Chem. Eng.*, 24 (2016) 1369–1374.
- [22] Y. Smaoui, M. Chaabouni, S. Sayadi, J. Bouzid, Coagulation-flocculation process for landfill leachate pretreatment and optimization with response surface methodology, *Desal. Water Treat.*, 57 (2016) 14488–14495.
- [23] M. Verma, R.N. Kumar, Coagulation and electrocoagulation for co-treatment of stabilized landfill leachate and municipal wastewater, *J. Water Reuse Desal.*, 8 (2018) 234–243.
- [24] Y. Zahrim, I. Azreen, S.S. Yoiing, J. Felijia, H. Hasmilah, C. Gloriana, I. Khairunis, Nanoparticles enhanced coagulation of biologically digested leachate, *Nanotechnol. Water Wastewater Treat.*, 11 (2019) 205–241, doi: 10.1016/B978-0-12-813902-8.00011-3.
- [25] W. Chen, P. Westerhoff, J.A. Leenheer, K. Booksh, Fluorescence excitation-Emission matrix regional integration to quantify spectra for dissolved organic matter, *Environ. Sci. Technol.*, 37 (2003) 5701–5710.
- [26] W. Chen, C. He, Z. Gu, F. Wang, Q. Li, Molecular-level insights into the transformation mechanism for refractory organics in landfill leachate when using a combined semi-aerobic aged refuse biofilter and chemical oxidation process, *Sci. Total Environ.*, 741 (2020) 2–7, doi: 10.1016/j.scitotenv.2020.140502.
- [27] W. Chen, C. He, X. Zhuo, F. Wang, Q. Li, Comprehensive evaluation of dissolved organic matter molecular transformation in municipal solid waste incineration leachate, *Chem. Eng. J.*, 400 (2020) 4–7, doi: 10.1016/j.cej.2020.126003.
- [28] L. Wang, F. Wu, R. Zhang, W. Li, H. Liao, Characterization of dissolved organic matter fractions from Lake Hongfeng, Southwestern China Plateau, *J. Environ. Sci.*, 21 (2009) 581–588.
- [29] H. Wang, Z. Cheng, Z. Sun, N. Zhu, H. Yuan, Z. Lou, X. Chen, Molecular insight into variations of dissolved organic matters in leachates along China's largest A/O-MBR-NF process to improve the removal efficiency, *Chemosphere*, 243 (2020) 2–7, doi: 10.1016/j.chemosphere.2019.125354.
- [30] Y. Zegzouti, A. Boutafda, A. Ezzariai, L.E. Fels, M.E. Hadek, M. Hafidi, Bioremediation of landfill leachate by *Aspergillus flavus* in submerged culture: evaluation of the process efficiency by physicochemical methods and 3D fluorescence spectroscopy, *J. Environ. Manage.*, 255 (2020) 1–8, doi: 10.1016/j.jenvman.2019.109821.
- [31] T. Zhang, J. Lu, J. Ma, Z. Qiang, Fluorescence spectroscopic characterization of DOM fractions isolated from a filtered river water after ozonation and catalytic ozonation, *Chemosphere*, 71 (2008) 911–921.
- [32] G.C. Zhu, C. Wang, X.W. Dong, Fluorescence excitation-emission matrix spectroscopy analysis of landfill leachate DOM in coagulation-flocculation process, *Environ. Technol.*, 38 (2017) 1489–1497.
- [33] H. Xu, M. Xu, Y. Li, X. Liu, L. Guo, H. Jiang, Characterization, origin and aggregation behavior of colloids in eutrophic shallow lake, *Water Res.*, 142 (2018) 176–186.
- [34] F. Jiang, B. Qiu, D. Sun, Advanced degradation of refractory pollutants in incineration leachate by UV/peroxymonosulfate, *Chem. Eng. J.*, 349 (2018) 338–346.